Progress Report

E.A. Heaphy[1]

Abstract

This report contains an overview of the work that has been done in multijet photoproduction analysis. A Hztool routine has been written that reproduces distributions of topological multijet variables for three-jet events using the PYTHIA event generator. The usefulness of HzTool for comparing data to analysis is discussed and the technique explained. There is also a discussion on correction factors, and finally a summary of future plans.

[1]University College London

Contents

1 Introduction

The first five to six months of the course were largely spent attending lectures and getting to grip with various analysis related tools. An exam project was completed which involved modelling the decay of D0 mesons using the Monte Carlo (MC) technique. This experience was usefull when it came to writing a dummy MC routine to demonstrate the correct use of correction factors, work which was used in a ZEUS note. The remainder of time has been spent researching photoproduction, and in particular multijet photoproduction. A HzTool subroutine was written to reproduce published multijet photoproduction cross sections. The bulk of this report is an overview of multijet photoproduction, with some space spared to explain HzTool and correction factors.

2 HERA/ZEUS Detector

HERA is the world's first lepton-proton collider, 6.3km in circumference and situated in Hamburg, Germany. It was designed to have an electron beam energy of 30 GeV and a proton beam energy of 820 GeV. In practice the electron energy is 27.52 GeV, giving a centre of mass energy $\sqrt{s} \simeq 300$ GeV.

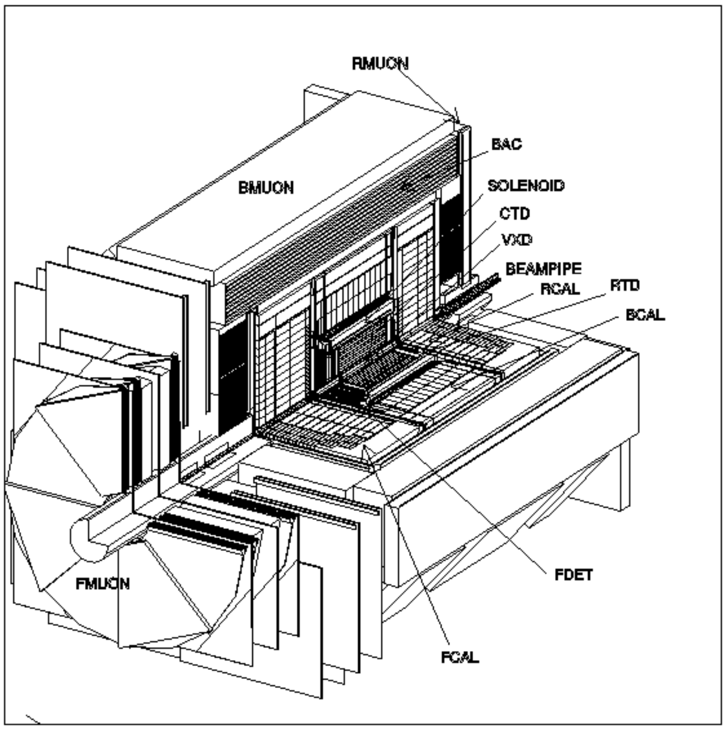

Figure 1: The ZEUS Detector

ZEUS, like H1, is a large general purpose detector built for HERA. It is situated at the south interaction point, and is shown in Figure 1, with the main features labelled.

The central tracking detector (CTD) was built by the UK, and together with the vertex detector (VXD) and the planar drift chambers, it tracks charged particles. Encasing the solenoid is a uranium-scintillator calorimeter (CAL) which is physically made of three parts: the forward, barrel and rear calorimeters (FCAL,BCAL and RCAL respectively). Although the CAL is not *strictly* hemetic, it does cover around 99.7% of the solid angle. This corresponds to a range in θ, the polar angle, of 2.6° to 176.1°. At HERA, pseudorapidity η is defined as:

$$\eta = -ln\ \ tan(\theta/2)$$

And the coverage of CAL in η is as follows:

FCAL:	$4.3 > \eta > 1.1$
BCAL:	$1.1 > \eta > -0.75$
RCAL:	$-0.75 > \eta > -3.8$

The CAL is a compensating uranium calorimeter, which means that the pulse heights of electrons and hadrons are equal to within 3% for momenta above 3 GeV/c. The energy resolution is $\sigma/E = 18\%\sqrt{E}$ for electrons, and $\sigma/E = 35\%\sqrt{E}$ for hadrons.

More detailed descriptions of the ZEUS detector and its components are given in [1] and [2].

3 HzTool

Analyses presented at HERA generally make use of particular Monte Carlo generators and apply specific cuts. When another physicist wishes to compare their results with similar studies they can be hindered by an inconsistency in their MC generators and cuts. HzTool is a library of generic routines which reproduce a comprehensive collection of data published by ZEUS and H1. It enables direct comparison between data and different experimental distributions by making it easy to alter cuts, generators and PDF's etc.

The HZ98001.f routine was written to allow comparison of three-jet photoproduction data from ZEUS with predictions from several different event generators. So far, this has only been done with PYTHIA [3].

4 Multijet Photoproduction

4.1 Dijet Photoproduction

Kinematics

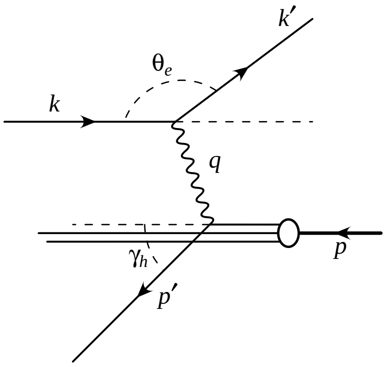

Figure 2: Kinematics at HERA

The kinematics for a simple electron-proton interaction producing a hadronic final state is shown in Figure 2. The four momenta of the interacting particles are denoted k,k',p, and q.

$k = (E_e, \vec{k})$
$k' = (E'_e, \vec{k'})$
$p = (E_p, \vec{p})$
$q = (E_\gamma, \vec{q})$

The square of the c.m.s energy is s:

$s = (k + p)^2$

Any two of the three Lorenzt invariant quantities below can be used to completely describe the kinematics of the lepton at fixed s.

$$Q^2 = -q^2 = (k' - k)^2 \tag{1}$$

$$y = \frac{q \cdot p}{k \cdot p} \tag{2}$$

$$x = -\frac{q^2}{2P \cdot q} \tag{3}$$

Expanding y gives:

$$y = \frac{E_p E_\gamma - \vec{q} \cdot \vec{p}}{E_e E_p - \vec{p} \cdot \vec{k}} \tag{4}$$

In the proton rest frame $\vec{p} = 0$, and therefore $y = E_\gamma / E_e$. This means that y is the fraction of electron beam energy carried by the photon in the proton rest frame. Also x can be thought of as the fraction of the proton's momentum that enters the hard scatter.

The virtuality of the photon is expressed by the value of Q^2, the negative square of the momentum transfer. In photoproduction the photon is nearly real, and the experimental cut off for such events is at $Q^2 < 1$ GeV. In photon exchange, the cross-section falls off rapidly, approximately as $\sim 1/Q^4$, with increasing Q^2, and so low Q^2 processes dominate.

To perform calculations, pQCD requires a large (hard) scale that is characteristic of the interaction, possibly invariant mass. When Q^2 is large it is used, for example in deep inelastic scattering (DIS). However, in photoproduction events Q^2 is unsuitable, and the transverse momentum of the jets provides the hard scale. By definition, hard scale is present in hard photoproduction events, allowing individual quarks and gluons to be resolved.

Experimentally, an event which has two or more high E_T jets is tagged as a hard photoproduction event if the positron is not detected in the calorimeter. This corresponds to a scattering angle of $\theta > 176.5°$ and $Q^2 \lesssim 1GeV^2$.

These constraints are designed to remove other events such as DIS and soft photoproduction from the signal. In soft photoproduction, there are no high E_T jets, and in DIS $Q^2 > 1GeV^2$.

At leading order QCD, two high E_T jets are produced in photon-proton collisions. This can can happen in two ways: direct or resolved processes.

Direct

There are three LO direct process shown in Figure 3: the first two are QCD compton scattering, and the last is boson-gluon fusion. In all cases the photon interacts directly with a gluon or quark from the proton. In the final state there are two jets and a proton remnant. The variable x_γ is the fraction of the photon's momentum that enters into the hard scatter. In direct processes it is equal to one.

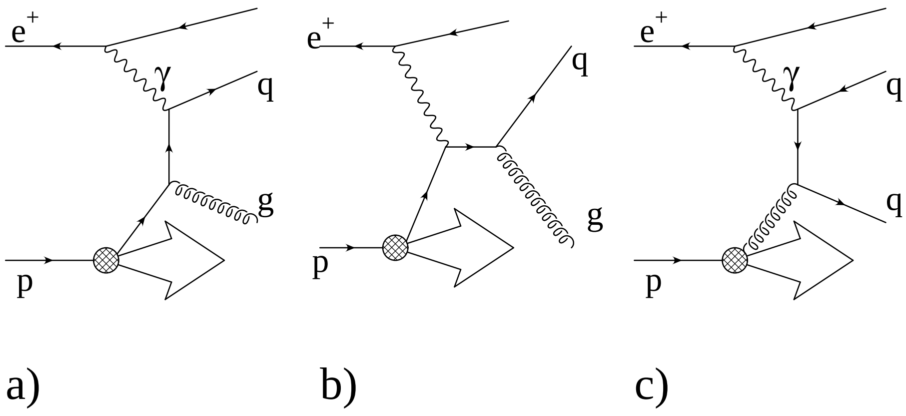

Figure 3: Direct subprocesses: a) and b) are QCD compton scattering, c) boson-gluon fusion

Resolved

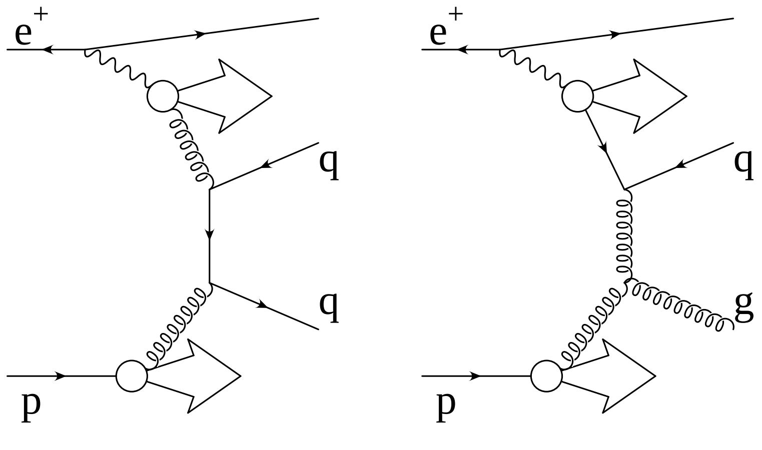

Figure 4: Examples of LO Resolved Photoproduction

There are many more diagrams for resolved processes at leading order than direct, two of which are shown in Figure 4 The photon fluctuates into a hadronic state providing partons which scatter from the proton partons. Therefore only a fraction of the photons momentum, x_γ, participates in the hard scatter. Unlike direct processes, there is a photon remnant in the final state which continues approximately in the original photon direction.

The variable x_γ^{OBS} is used to separate direct and resolved processes at all orders [4]. A general definition is given in equation (5), where $njets$ is the number of jets in the final state. At LO x_γ^{OBS} is the same as x. At higher orders the difference between x_γ^{OBS} and x becomes more pronounced. This is because there is blurring in definition between say, a resolved two-jet event and a direct 3-jet event.

$$x_\gamma^{OBS} = \frac{\sum_{i=1}^{i=njets} E_T^{jet_i} e^{-\eta^{jet_i}}}{2yE_e} \tag{5}$$

For a dijet event, $njets = 2$ and x_γ^{OBS} is the fraction of the photon's momentum used in the production of the two highest transverse energy (E_T) jets.

4.2 Jet Definition

The quarks and gluons produced in the final state of any process cannot be directly detected due to QCD confinement. A stream of particles evolve from them instead, called a parton shower or jet, which hadronises before entering the detector.

However, the energy and direction of the initial partons are expected to be preserved in high energy jets. Therefore the topology of the partons in the initial parton system can be deduced from the final state jet topology.

The definition of a jet is not trivial, as it is not a QCD object. It is defined by the type of algorithm or jet finder used. In hadron-hadron physics cone algorithms are normally used to define jets because of the ease with which proton remnants can be factorised out. Examples of cone algorithms used in ZEUS are PUCELL and EUCELL.

In the multijet analysis described here a cluster algorithm, KTClUS [5, 6], is used.Although most cluster algorithms were designed for e^+e^- experiments in the past [7], newer versions have overcome previous problems of remnant treatment.

To compare prediction with data, an event generator is used that models the parton shower and hadronisation stages. Here PYTHIA is used, but other common generators are HERWIG and NJETS. They simulate events by calculating the matrix element for the required subprocess, and effectively weighting it according to a given parton distribution function (PDF). PDF's are functions which express the most probable effective content of the proton at a given Q^2 and x.

Results from experiment and data are compared at the hadron level largely because it does not require as much MC modelling as a comparison at, say, the parton level would involve.

4.3 Dynamics of Multijet Photoproduction

Introduction

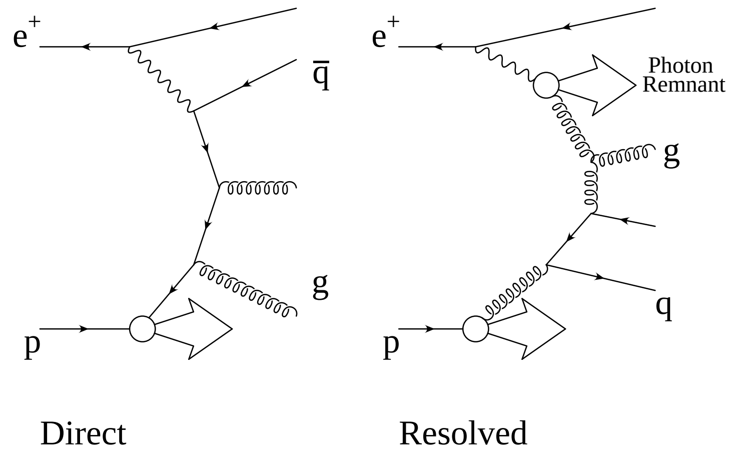

Figure 5: Three-Jet Photoproduction

The next to leading order (NLO) diagrams for hard photoproduction involve processes in which there are three jets present in the final state. As at leading order, this can happen via both direct and resolved processes. Figure 5 showss two tree-level diagrams for 3-jet photoproduction.

At the Tevatron, the CDF [8, 9] and D0 [10] collaborations have extensively studied multijet events arising from proton-antiproton interactions. This examines the properties of strong interactions at short distances and order α_s^3.

To date, studies of high-mass multijet events have been compared with predictions from:the LO QCD matrix element, QCD parton shower MCs, and phase-space models. In phase-space the coordinates represent the variables required to specify the state of the system. The model fills this space uniformly with events, ie in a manner which disregards any physics that have might occurred.

Further motivation for gaining a detailed understanding of these events, is that when high luminosity colliders such as LHC start running multijet event production is expected to be prolific. It is also possible that the study could uncover new phenomena, or exotic processes that have multijets in the final state.

At HERA, the ZEUS collaboration have recently measured the cross sections for the photoproduction of three of more high transverse energy jets. The analysis was performed on data taken in the 1995 - 96 running period, with a luminosity of around 16 pb^{-1}. The data shown in Figure 10 are from distributions produced in the analysis of three-jet photoproduction of order $\alpha\alpha_s^2$ performed by E.Strickland and L.Sinclair. Compared to this data are MC predictions produced by a Hztool routine using PYTHIA.

Definition of Variables

The variables defined below and used in the analysis discussed here were first proposed by Geer and Asakawa [11]. They argued that these variables make it easy to compare the characteristics of events with different numbers of jets in the final state. Also, the variables span the multijet parameter space and are in theory easy to relate to pQCD predictions.

To completely specify a system of N-jets in the final state, (4N-3) variables are required. However, in practice only (4N-4) are used. This is because the system can be rotated about the beam direction without losing any interesting information. Figure 6 shows a table listing the variables used to describe 2, 3, 4, 5 and 6 jet systems.

Variables are defined in the N-jet centre of mass (c.m.s) frame. A schematic definition of these variables in a 3-jet rest frame are shown in Figure 7. By convention, the two incoming partons are labelled 1 and 2. The outgoing jets are labelled in descending c.m.s energy 3,4 and 5, such that:

$$E_3 > E_4 > E_5$$

Four dimentionless variables are used to described a system with fixed 3-jet c.m.s energy : X_3, X_4, $cos\theta_3$ and ψ_3.

$$X_3 = \frac{2E_3}{M_{345}} \tag{6}$$

$$X_4 = \frac{2E_4}{M_{345}} \tag{7}$$

$$cos\theta_3 = \frac{\vec{P}_{AV} \cdot \vec{P}_3}{|\vec{P}_{AV}||\vec{P}_3|} \tag{8}$$

Two-Jet	Three-Jet	Four-Jet	Five-Jet	Six-Jet
m_{2J} $\cos\theta^*$ f_3 f_4	m_{3J} $\cos\theta_3$ f_3 f_4	m_{4J} $\cos\theta_{3'}$ $f_{3'}$ $f_{4'}$	m_{5J} $\cos\theta_{3''}$ $f_{3''}$ $f_{4''}$	m_{6J} $\cos\theta_{3'''}$ $f_{3'''}$ $f_{4'''}$
	f_5 ψ_3 X_3 X_4	$f_{5'}$ $\psi_{3'}$ $X_{3'}$ $X_{4'}$	$f_{5''}$ $\psi_{3''}$ $X_{3''}$ $X_{4''}$	$f_{5'''}$ $\psi_{3'''}$ $X_{3'''}$ $X_{4'''}$
		f_A f_B X_A ψ'_{AB}	$f_{A'}$ $f_{B'}$ $X_{A'}$ $\psi''_{A'B'}$	$f_{A''}$ $f_{B''}$ $X_{A''}$ $\psi'''_{A''B''}$
			f_C f_D X_C ψ''_{CD}	$f_{C'}$ $f_{D'}$ $X_{C'}$ $\psi'''_{C'D'}$
				f_E f_F X_E ψ'''_{EF}

Figure 6: Table of variables used in multijet photoproduction

$$\psi_3 = \frac{(\vec{P}_3 \times \vec{P}_{AV}) \cdot (\vec{P}_4 \times \vec{P}_5)}{|\vec{P}_3 \times \vec{P}_{AV}| \cdot |\vec{P}_4 \times \vec{P}_5|} \tag{9}$$

Where M_{345} is the 3-jet c.m.s energy and $\vec{P}_{AV}$ is the average beam direction. The three momentums of partons 3, 4 and 5 are labelled $\vec{P}_3$, $\vec{P}_4$, and $\vec{P}_5$ respectively. The cosine of the polar angle of the leading jet w.r.t to the beam is denoted $cos\theta_3$. Due to conservation of momentum, the three jets are contained in the same plane in the 3-jet c.m.s. The angle this plane makes with one formed by $\vec{P}_{AV}$ and the leading jet is defined as ψ_3.

A third Dalitz variable, X_5, is defined in the same way as X_3 and X_4. By definition the sum of these variables equals two, as each is twice the fraction of avaiable energy taken by each jet.

In addition, there are the single-jet mass fractions, where j= 3 ... 5:

$$F_j = \frac{M_j}{M_{345}} \tag{10}$$

Extending the variables to four and five jet events is relatively straightforward. Four-jet systems are reduced to three-body systems by combining the two jets with the lowest two-jet masses. The treatment of a five-jet system is to reduced it to a

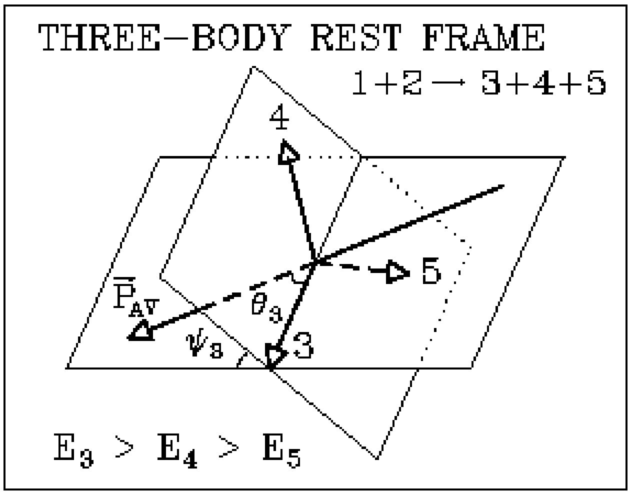

Figure 7: Variables defined in three-jet c.m.s

four-jet and then three-jet system. Thus systems with different numbers of jets in the final stage can be compared.

Discussion of Cuts

An account of the cuts used in the 3-jet photoproduction analysis at HERA follows. The cuts used to produce the data were also used to produce the MC predictions.

A cut on y, $0.2 < y < 0.8$, was implemented to reduce background.This background emanates from contamination from beam gas and cosmic ray events, plus non-photoproduction events. More explicitly, DIS events where an electron passes through the ecal undetected can be removed by the upper cut on y. In this case the absence of lepton may otherwise be falsely labelled a photoproduction event , but $y \simeq 1$ GeV and so it is not a photoproduction event.

The events which passed the cuts were required to have at least three jets with $E_T^{jet} > 6$ GeV and $\eta^{jet} < 2.5$. Low E_T events dominate the cross-section, but as $E_T \rightarrow 0$ these soft photoproduction events cannot be described by pQCD. The intention is to maximise the number of available statistics while obtaining a cross section which is peturbatively calcuable.

However this cut off in E_T affects the $cos\theta_3$ distribution. Events with the leading jet close to the beam axis, and hence low E_T, have $|cos\theta_3|$ values approaching 1. There is also a tendency for events with a leading jet with low E_T to have low M_{345}. To minimise the effect of the E_T cut on the $cos\theta_3$ distribution it is required that $M_{345} > 50$GeV and $|cos\theta_3| < 0.8$. Figure 8 shows that this is a sensible region of data to use.

In addition it is required that $X_3 < 0.95$ to increase the energy available to the third jet. Due to energy conservation, the range of values the Dalitz variables can have are:

$2/3 < X_3 < 1$
$1/2 < X_4 < 1$
$0 < X_5 < 2/3$

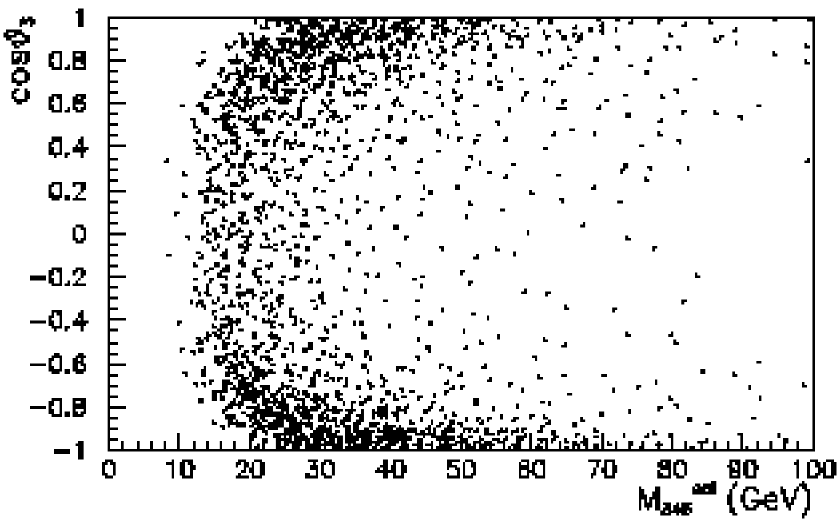

Figure 8: $cos\theta_3$ vs M_{345} for three jet events passing the E_T^{jet} and η^{jet} cuts.

Some Results For 3-Jet Distributions

Results from the CDF collaboration [9, 8] indicate that the M_{345} and $cos\theta_3$ distributions are approximately independent of jet multiplicity and are well described by HERWIG, a parton shower MC event generator. Also, parton-level QCD calculations agree well with data for 3, 4 and 5-jet events. This suggests that $2 \rightarrow 2$ scattering plus gluon radiation are a good first approximation to the full LO QCD matrix elements for multijets. Phase space models on the other hand are largely unsuccessful at describing the data, and this reaffirms the validity of QCD calculations.

The plots in Figure 10 show the 3-jet photoproduction analysis on data obtained from the ZEUS detector. The first plot shows how the three-jet invariant mass distribution falls off rapidly. Most of the events populate the low M_{345}, low E_T region. The shape of the $cos\theta_3$ distribution reflects this also.

The ψ_3 distribution is flatter, but shows peaks towards 0 and π, indicating a tendency for the plane containing the second and third jet to line up with the plane containing the first jet and the beam direction. This characteristic is related to colour coherence.

The X_3 and X_4 plots indicate that the fraction of available 3-jet c.m.s energy taken by the first two jets peaks at about 0.95 and 0.68 respectively.

The MC event generator, PYTHIA, shown as a band, reproduces the shape of the data well. However, the cross-sections are significantly lower than data. This is shown in the M_{345} plot which has not been area renormalised. The PDF's used to make these plots were GRV LO for the photon, and CTEQ 4L for the proton. In the last zone of Figure 10 is shown a plot comparing the cross-sections for ψ_3 using these PDF's (black band) and a different set (grey band). The PDF's in the grey band are GRV-G set L-HO for the photon, and MRS(A) for the proton.

It is commonly believed that the PDFs do not significantly alter the height of the cross-sections, but in this case, at least, this assumption is clearly wrong. The cross-section is significantly increased by a change in PDF selection, and this is demonstrated more clearly by Figure 9. The cross-section in the lower plot is within the error bars of the data for a number of points.

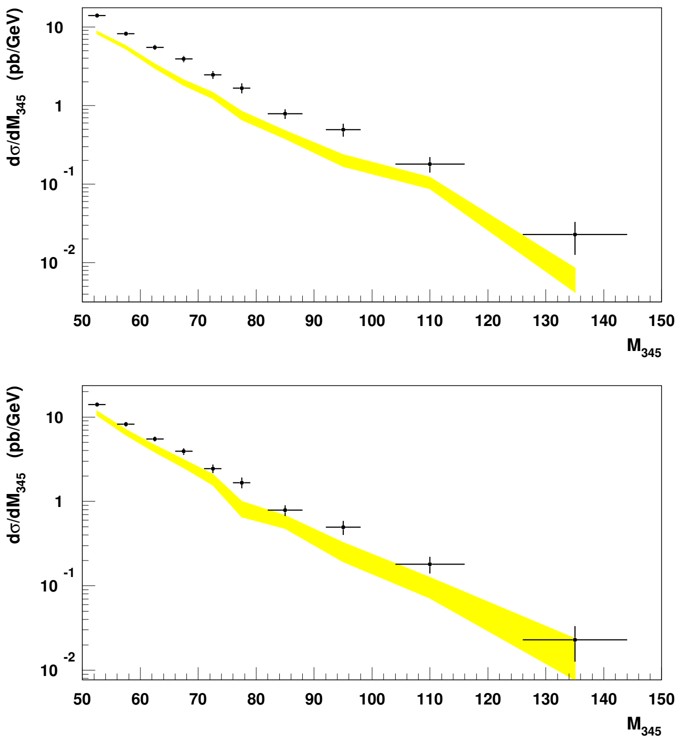

Figure 9: Absolute normalisation cross-sections for M_{345} using different PDFs: top)GRV LO and CTEQ 4L, bottom) GRV-G L-HO and MRS(A) for the photon and proton respectively.

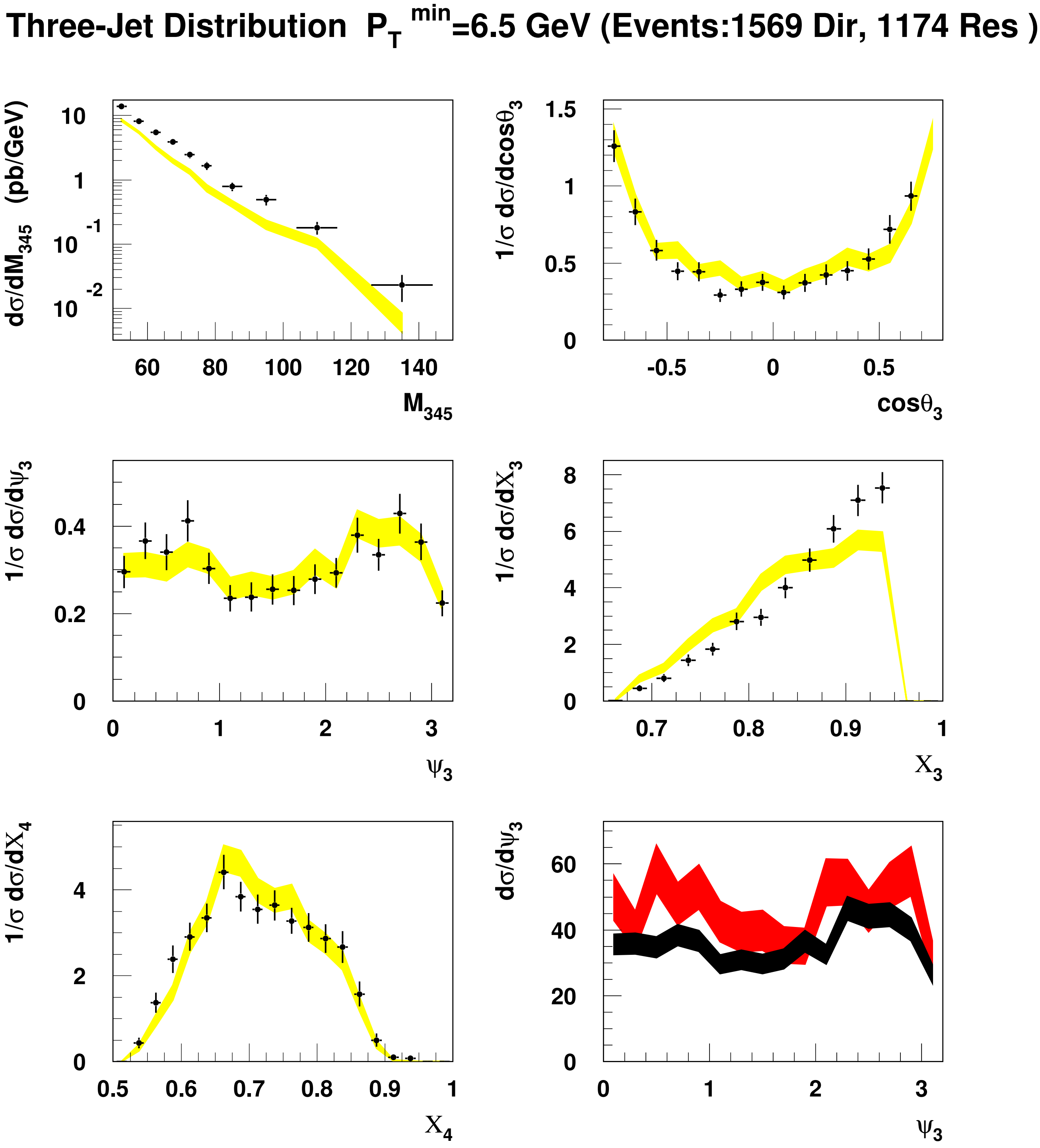

Figure 10: ZEUS data compared with PYTHIA using HzTool

5 Correction Factors

A toy MC routine was written to demonstrate the validity of a certain energy correction method. A detailed discussion of this topic is found in [13] which includes the plots produced using this toy MC.

6 Future Plans

Future plans involve working on photon parton distribution functions, initially at leading order for photoproduction. Eventually this will be extended to NLO and DIS events.

References

[1] ZEUS Collaboration; *Phys. Lett.* B **293**, 465 (1992)

[2] The ZEUS Detector Status Report 1993, DESY 1993.

[3] H.U. Bengtsson and T. Sjostrand, *Comp. Phys. Comm.***46**(1987);T.Sjostrand, CERN-TH.6488/92,(1992)

[4] ZEUS Collaboration.,M. Derrick *et al*,. *Phys. Lett.* B **348**, 665 (1995)

[5] S.Catani, Yu.L.Dokshitzer, M.H. Seymour and B.R. Webber, *Nucl. Phys.* B**406**,187 (1993)

[6] S. Catani, Yu.L. Dokshitzer and B.R. Webber;*Phys. Lett.* B **285**, 291 (1992)

[7] JADE Collaboration, *Phys. Lett.*, B 213:235 (1988)

[8] CDF Collaboration, F. Abe *et al.*,*Phys. Rev. Lett.* **75**, 608 (1995)

[9] CDF Collaboration, F. Abe *et al.*,*Phys. Rev.* D **54**, 4221 (1996)

[10] D0 Collaboration, S. Abachi *et al.*,hep-ex/9509005 v2 12 Sep 1995

[11] T. Asakawa and S. Geer, *Phys. Rev.* D **53**, 4793 (1996).

[12] ZEUS Collaboration, J. Breit *et al.*,*Eur. Phys. J.* C **1**, 109 (1998)

[13] J.M. Butterworth, E. A. Heaphy and M. R. Sutton; ZEUS-98-032